

Improvement in Making ACI-rat Model of Hepatocellular Carcinoma in The Experiments of Interventional Therapy and Its Imaging Properties

SuSu Zheng

liver cancer institute and zhongshan hospital <https://orcid.org/0000-0003-3993-2377>

ChangJun Tan

liver cancer institute

JiaJia Lin

liver cancer institute

ChuYu Jing

liver cancer institute

Xin Yin

liver cancer institute

JinWu Hu

liver cancer institute

Hui Tan

Department of Nuclear medicine

Boheng Zhang (✉ zhang.boheng@zs-hospital.sh.cn)

Zhongshan Hospital and Shanghai Medical School, Fudan University

Research

Keywords: Hepatocellular carcinoma, ACI-rat model, Transarterial chemoembolization, Imaging properties

Posted Date: September 3rd, 2020

DOI: <https://doi.org/10.21203/rs.3.rs-67779/v1>

License: © ⓘ This work is licensed under a Creative Commons Attribution 4.0 International License.

[Read Full License](#)

Abstract

PURPOSE

To improve the preparation of August Copenhagen Irish(ACI)-rat model suitable for interventional therapy, and to investigate its ^{18}F -2-fluoro-2-deoxy-D -glucose-Positron emission tomography(FDG-PET) and magnetic resonance imaging(MRI) features.

METHODS

Morris hepatoma 3924A tumors were implanted in the left lobe of the liver in 20 male ACI rats. FDG-PET and MRI scans were performed on day 14 after implantation. After that, all the rats were sacrificed and samples of tissues were fixed and used for various analyses.

RESULTS

FDG-PET scans showed increased uptake of ^{18}F -FDG of tumor nodules, and no signs of wound and peritoneal cavity metastases. The average maximum standardized uptake value(SUVmax) in tumors was 4.85 ± 0.86 (range, 3.58–6.6) and 0.79 ± 0.42 (range, 0.27–1.63) in the surrounding normal liver tissues. Tumor nodules on MRI were shown to be hypointensity on T1-weighted images and hyperintensity on T2-weighted images. The average tumor volume was $106 \pm 15 \text{ mm}^3$. No intrahepatic metastasis or lung metastasis were found on day 14.

CONCLUSION

FDG-PET is useful in screening the earlier cases with implantation metastasis. MRI is useful in assessing this interventional model. The tumor model shows a well application for the interventional therapy experiment.

Introduction

Hepatocellular carcinoma (HCC) is a common malignancy, which is the third leading cause of death in cancer-related disease[1, 2]. Liver transplantation and radical resection is the currently accepted treatment of choice in patients who have early stage HCC[3]. The majority of patients present with multiple tumors or portal vein tumor invasion are treated with transarterial chemoembolization (TACE), and recent guidelines recommend TACE for those selected patients as a first-line treatment[4, 5]. TACE, which selectively obstructs the tumor vessels, is conventionally performed by intra-arterial infusion of lipiodol or microspheres, along with chemotherapeutics[6]. However, as patients with advanced HCC treated by TACE vary tremendously in prognosis, the most valuable treatment modality of TACE deserves

exploring[7, 8]. Thus, establishing suitable animal experiments mimicking the clinical procedures of TACE therapy are a pressing need. The Morris hepatoma 3924A tumor model in August Copenhagen Irish(ACI) rats has been shown to have a high degree of similarity with human HCC, which has been proved to be hypervascular and mainly supplied by hepatic artery. More importantly, the tumor is demonstrated to be a poorly differentiated HCC verified by pathology and exhibits the possible usage in the study of TACE[9–12]. However, by adopting the tumor implantation technique described by Trubenbach J[9], implantation metastasis in the peritoneum was easily to be observed. We improved the tumor implantation technique by using a small piece of adipose tissue covering the wound surface and then stitched the wound. Besides, many experimental studies have shown increased uptake of ^{18}F -2-fluoro-2-deoxy-D –glucose in malignant tumors with increased glucose utilization. Metabolic imaging of tumors by FDG-PET may be useful in detecting recurrences and evaluating therapeutic effects[13–15]. So far, experimental TACE model of ACI rats have not previously been evaluated by ^{18}F -FDG-PET. The goal of this study was to improve the preparation of ACI -rat TACE model and investigate its ^{18}F -2-fluoro-2-deoxy-D-glucose-Positron emission tomography(FDG-PET) and magnetic resonance imaging(MRI) features.

Materials And Methods

Animals and tumor cell line

A total of 20 male ACI rats (Slac Laboratory Animal Company, Shanghai) weighing $260\pm 20\text{g}$ were used in this research. A rat HCC cell line Morris hepatoma 3924A with a rapidly growing characteristics was applied in this study[9]. The study was approved by our institutional review board.

Anesthesia

All the animals were anesthetized with 1% pentobarbital sodium (30 mg/ kg body weight) injection in the interventional procedures and isoflurane in all imaging procedures.

Liver implantation

Liver tumor implantation was performed according to a modification procedures reported by Trubenbach J et al.[9]. Briefly, 1×10^7 Morris 3924A cells were injected subcutaneously into one ACI rat to develop implantation tumor. Two weeks later, the tumor-bearing rat was sacrificed and the solid tumor was extracted and diced into small pieces with a tumor volume of about 2mm^3 . Then another 20 ACI rats were anesthetized and received an open abdominal surgery. Tumor fragment implantation was performed under microscope with microsurgical forceps and scissors. In short, a 1cm length of subcapsular incision was made with the forceps and then the 2mm^3 tumor cubes were inserted into the left lateral lobe of the liver. An eight suture was carefully done for closing the wound, together with a piece of adipose tissue covering the wound surface. After that, the abdominal wall was closed (Fig. 1).

Imaging analysis

FDG-PET and MR imaging were performed by using a PET/MR unit (PET/MR; Metis). On day 14, 20 tumor-bearing rats were anesthetized after 12 hr of fasting with sodium pentobarbital. Then the rats received an intravenous injection of ^{18}F -FDG through the caudal vein (2.4-3.2 MBq/kg). The time of commencement of injection was defined as time 0. One bed position that included the heart to the abdomen was imaged. Dynamic PET images were obtained with an animal PET camera at time 60-90 min. MR imaging was also performed for analyzing tumor sizes. The section thickness was set as 3 mm for both T1-weighted images and T2-weighted images. Section gap was set as 1 mm, we did not use any contrast medium for all the examined animals. We measured the tumor volume in T2-weighted image and used the following formula: Tumor volume (mm^3) = largest diameter (mm) [smallest diameter (mm)]² / 2 [16].

Tissue evaluation

When the final MRI experiments were finished, all the animals were euthanized. The tumor-bearing liver was dissected, and after careful removal from the liver tissue, the tumors as well as the lung tissues were fixed in 5% formaldehyde solution for histological preparation. The tumor metastases rates were analyzed.

Results

Characteristics of the rat bearing tumor and histopathological findings

Tumor cubes of Morris hepatoma 3924A were successfully implanted in all 20 rat livers. No surgical-related death was observed in any of the given specimens. The mean tumor volume was $106 \pm 15 \text{ mm}^3$. Hematoxylin-Eosin (H&E) staining was performed, and the tumor sections implied a poorly differentiated HCC, which was characterized by large and abnormal nucleus, and mitotically active. The tumors were hardly distinguished from the peripheral normal tumor tissue because of no obvious capsule. The tumors were abundant with blood supply, small arteries and capillaries were easily to be seen. No intrahepatic metastasis or lung metastasis was detectable in any of the 20 rats (Fig. 2).

Tumor imaging

On day 14, FDG-PET were used in all 20 rats. Images were analyzed and maximum standardized uptake value (SUV_{max}) were given for all tested animals. The tumors showed an increased uptake of ^{18}F -FDG in PET imaging. The average SUV_{max} in rat tumors was 4.85 ± 0.86 (range, 3.58-6.6) and 0.79 ± 0.42 (range, 0.27-1.63) in the surrounding normal liver tissues. Only one single lesion with FDG positive accumulation was found in each of the rat liver (Fig. 3). By day 14, lesions in the livers was also detected by MRI, Tumor nodules implied by MRI were shown to be hypointensity on T1-weighted images and hyperintensity on T2-weighted images (Figs. 4A and 4B). Necrosis was not found in any of the lesions.

Discussion

TACE has been shown to be beneficial for selected patients with unresectable HCC[17], however several questions remain to be elucidated. There are large variations in survival reported after TACE[18]. TACE uses arterial obstruction as well as sustained chemotherapeutic effect to induce tumor necrosis. There are a variety of agents for embolization, such as microspheres, drug-eluting microspheres and lipiodol. Among them, lipiodol was widely accepted in Asia, especially in China. Until now, no embolic agent has been widely accepted and used by all hospitals for a lack of consensus. There is still no answers for the optimal treatment modality of TACE[19]. Therefore, a suitable animal model for TACE therapy will help resolving those issues.

The ACI-rat TACE model has proved to show a high reproducibility of tumor growth characteristics. The tumor showed weak metastatic potential and was abundant with blood supply, which was better than the tumor models of Walker-256 □Novikoff hepatoma or VX-2[20–22]. In the present study, we discovered that the model showed a good potential application prospect for TACE experiments. We concluded that the tumor around 14 days after implantation was suitable for further TACE treatment, as the tumor had proper size, hypervascularization and no evident of necrosis. Besides, the model was characterized by easy to operate and convenient to make and the successful rate of implantation was 100% (20/20).

Abdominal implantation metastasis was easily to be seen in this model in our preliminary experiment, especially around the wound of the liver. Here, in this study, we improved the tumor implantation technique described by Trubenbach J al.[9]. We fixed the tumor cube with a small piece of adipose tissue covering the wound surface and then stitched the wound, thus the tumor fragment was guaranteed to stay and grow just in the implantation site. Our method was proved to be helpful in avoiding artificial abdominal implantation metastasis. Here in this study, we observed no detectable peritoneal tumor and abdominal adhesion formation up to day 14 after implantation.

^{18}F -FDG can provide a useful indicator of tumor growth and metastasis because ^{18}F -FDG accumulates in tumor mass with increased glucose metabolism[15, 23]. Here, our data demonstrated that the tumors showed an increased uptake of ^{18}F -FDG in PET imaging which was markedly different from the surrounding liver tissues. Besides, only one single lesion with FDG positive accumulation was found. Thus, no sign of implantation metastasis was found at the beginning. FDG-PET may be useful for selecting proper candidates for further treatment of TACE. S.I. Park et al. have shown that FDG uptake serves as a good screening test to evaluate the feasibility of DEN-induced HCC in a rat liver tumor model[24]. Researchers have also indicated that FDG-PET could also be used for evaluating treatment efforts in animal liver cancer. On a rabbit VX2 liver tumor model, FDG uptake was significantly decreased after transcatheter arterial embolization(TAE) and radiotherapy. Thus FDG-PET was helpful for the early evaluation of the therapeutic effects on liver tumors[25, 26]. The aim of the present study was to improve the tumor implantation technique, introduce a noninvasive modality for monitoring the tumors growth and metastasis conditions and then selecting proper candidates for further TACE therapy. So we did not operate TACE and the usage of FDG-PET in evaluating the therapeutic effects of TACE was not investigated, which is absolutely one of the limitations of this study. This should be explored in further studies.

In the present research, MR imaging was also used to monitor tumor growth during the experimental period. With MR imaging we observed, as did Qian J et al.[12], the tumors were shown to be hypointensity on T1-weighted images and hyperintensity on T2-weighted images, which was similar to those of the human hepatocellular carcinoma. On day 14, the mean tumor size measured by MR imaging was $106 \pm 15 \text{ mm}^3$ and no necrosis was observed, which is similar to the results of the others[10]. Hence, the tumor has a proper growth rate and is suitable for further TACE treatment.

Although the ACI-rat TACE model has proven to be valuable employed in the animal research of TACE, some limitations remained. First, the tumor is still a fast-growing tumor and the average life span of the tumor bearing rats is short. It is not suitable for evaluating the long-term effect of TACE. Second, the Morris 3924A tumor shows little metastatic spread. In this study, we observed no peritoneal metastasis, satellite liver nodules or lung metastasis. Thus, this model may not be suitable for researches on the metastasis potential of residue tumor after TACE.

In conclusion, the ACI-rat TACE model shows similar characteristics of human HCC. FDG-PET and MR imaging are useful in optioning and evaluating the model. It is strongly recommended to be widely used in the study of TACE.

Abbreviations

HCC, hepatocellular carcinoma; TACE, transarterial chemoembolization; ^{18}F FDG-PET, 18F-2-fluoro-2-deoxy-D-glucose-Positron emission tomography; MRI, magnetic resonance imaging;

Declarations

Ethics approval and consent to participate

Animal use was approved by the Zhongshan hospital Animal Care Committee

Consent for publication

Not applicable

Availability of data and materials

The datasets used and/or analyzed during the current study are available from the corresponding author on reasonable request.

Competing interests

The authors declare that they have no competing interests.

Funding

This research was supported by grants from the National Natural Science Foundation of China (81173391) and the Shanghai Municipal Commission of Health and Family Planning(ZY3-CCCX-3-2004).

Authors' contributions

ZSS worked on the conception, design, acquisition, analysis, and interpretation of all data and was the primary author for the draft manuscript. TCJ assisted with animal model creation and H&E staining. LJJ assisted with study conception and manuscript revision. JCY, YX and HJW assisted with animal model creation. TH assisted with animal model creation and FDG-PET operation. ZBH is the senior author, overseeing all aspects of the study. All authors read and approved the final manuscript.

Acknowledgements

We thank Chen Jun, Dong Yingying, Xie Chenlong for their help with the animal experiments.

References

1. Ryerson AB, Ehemann CR, Altekruse SF, Ward JW, Jemal A, Sherman RL, Henley SJ, Holtzman D, Lake A, Noone AM, et al: Annual Report to the Nation on the Status of Cancer, 1975-2012, featuring the increasing incidence of liver cancer.*Cancer-Am Cancer Soc* 2016, 122:1312-1337. doi:10.1002/cncr.29936.
2. Ferlay J, Soerjomataram I, Dikshit R, Eser S, Mathers C, Rebelo M, Parkin DM, Forman D, Bray F: Cancer incidence and mortality worldwide: sources, methods and major patterns in GLOBOCAN 2012.*Int J Cancer* 2015, 136:E359-E386. doi:10.1002/ijc.29210.
3. Yang JD, Hainaut P, Gores GJ, Amadou A, Plymoth A, Roberts LR: A global view of hepatocellular carcinoma: trends, risk, prevention and management.*Nat Rev Gastroenterol Hepatol* 2019, 16:589-604. doi:10.1038/s41575-019-0186-y.
4. Llovet JM, Real MI, Montana X, Planas R, Coll S, Aponte J, Ayuso C, Sala M, Muchart J, Sola R, et al: Arterial embolisation or chemoembolisation versus symptomatic treatment in patients with unresectable hepatocellular carcinoma: a randomised controlled trial.*Lancet* 2002, 359:1734-1739. doi:10.1016/S0140-6736(02)08649-X.
5. Lo CM, Ngan H, Tso WK, Liu CL, Lam CM, Poon RT, Fan ST, Wong J: Randomized controlled trial of transarterial lipiodol chemoembolization for unresectable hepatocellular carcinoma.*Hepatology* 2002, 35:1164-1171. doi:10.1053/jhep.2002.33156.
6. Inchingolo R, Posa A, Mariappan M, Spiliopoulos S: Locoregional treatments for hepatocellular carcinoma: Current evidence and future directions.*World J Gastroenterol* 2019, 25:4614-4628. doi:10.3748/wjg.v25.i32.4614.
7. Sangiovanni A, Colombo M: Treatment of hepatocellular carcinoma: beyond international guidelines.*Liver Int* 2016, 36 Suppl 1:124-129. doi:10.1111/liv.13028.

8. Facciorusso A, Licinio R, Muscatiello N, Di Leo A, Barone M: Transarterial chemoembolization: Evidences from the literature and applications in hepatocellular carcinoma patients. *World J Hepatol* 2015, 7:2009-2019. doi:10.4254/wjh.v7.i16.2009.
9. Trubenbach J, Graepler F, Pereira PL, Ruck P, Lauer U, Gregor M, Claussen CD, Huppert PE: Growth characteristics and imaging properties of the morris hepatoma 3924A in ACI rats: a suitable model for transarterial chemoembolization. *Cardiovasc Intervent Radiol* 2000, 23:211-217. doi:10.1007/s002700010045.
10. Qian J, Vossoughi D, Woitaschek D, Oppermann E, Bechstein WO, Li WY, Feng GS, Vogl T: Combined transarterial chemoembolization and arterial administration of Bletilla striata in treatment of liver tumor in rats. *World J Gastroenterol* 2003, 9:2676-2680. doi:10.3748/wjg.v9.i12.2676.
11. Maataoui A, Qian J, Vossoughi D, Khan MF, Oppermann E, Bechstein WO, Vogl TJ: Transarterial chemoembolization alone and in combination with other therapies: a comparative study in an animal HCC model. *Eur Radiol* 2005, 15:127-133. doi:10.1007/s00330-004-2517-8.
12. Wang S, Dunlap TL, Huang L, Liu Y, Simmler C, Lantvit DD, Crosby J, Howell CE, Dong H, Chen SN, et al: Evidence for Chemopreventive and Resilience Activity of Licorice: Glycyrrhiza Glabra and G. Inflata Extracts Modulate Estrogen Metabolism in ACI Rats. *Cancer Prev Res (Phila)* 2018, 11:819-830. doi:10.1158/1940-6207.CAPR-18-0178.
13. Colin DJ, Bejuy O, Germain S, Triponez F, Serre-Beinier V: Implantation and Monitoring by PET/CT of an Orthotopic Model of Human Pleural Mesothelioma in Athymic Mice. *J Vis Exp* 2019. doi:10.3791/60272.
14. Li P, Liu Q, Wang X, Huang G, Song S: 18F-Deoxyglucose (18F-FDG) Positron Emission Tomography/Computed Tomography (PET/CT) Monitoring of Dynamic Growth Characteristics of Walker-256 Tumor Models in 3 Different Locations in Rats. *Med Sci Monit* 2019, 25:558-564. doi:10.12659/MSM.909286.
15. Liu S, Feng Z, Wen H, Jiang Z, Pan H, Deng Y, Zhang L, Ju X, Chen X, Wu X: (18)F-FDG PET/CT can predict chemosensitivity and proliferation of epithelial ovarian cancer via SUVmax value. *Jpn J Radiol* 2018, 36:544-550. doi:10.1007/s11604-018-0755-y.
16. Carlsson G, Gullberg B, Hafstrom L: Estimation of liver tumor volume using different formulas - an experimental study in rats. *J Cancer Res Clin Oncol* 1983, 105:20-23. doi:10.1007/BF00391826.
17. Huo YR, Eslick GD: Transcatheter Arterial Chemoembolization Plus Radiotherapy Compared With Chemoembolization Alone for Hepatocellular Carcinoma: A Systematic Review and Meta-analysis. *Jama Oncol* 2015, 1:756-765. doi:10.1001/jamaoncol.2015.2189.
18. Forner A, Llovet JM, Bruix J: Chemoembolization for intermediate HCC: is there proof of survival benefit? *J Hepatol* 2012, 56:984-986. doi:10.1016/j.jhep.2011.08.017.
19. Yang B, Liang J, Qu Z, Yang F, Liao Z, Gou H: Transarterial strategies for the treatment of unresectable hepatocellular carcinoma: A systematic review. *Plos One* 2020, 15:e227475. doi:10.1371/journal.pone.0227475.

20. Li X, Zheng CS, Feng GS, Zhuo CK, Zhao JG, Liu X: An implantable rat liver tumor model for experimental transarterial chemoembolization therapy and its imaging features. *World J Gastroenterol* 2002, 8:1035-1039. doi:10.3748/wjg.v8.i6.1035.
21. NOVIKOFF AB: A transplantable rat liver tumor induced by 4-dimethylaminoazobenzene. *Cancer Res* 1957, 17:1010-1027.
22. Chen JH, Lin YC, Huang YS, Chen TJ, Lin WY, Han KW: Induction of VX2 carcinoma in rabbit liver: comparison of two inoculation methods. *Lab Anim* 2004, 38:79-84. doi:10.1258/00236770460734434.
23. Kutluturk K, Simsek A, Comak A, Gonultas F, Unal B, Kekilli E: Factors affecting the accuracy of (18)F-FDG PET/CT in evaluating axillary metastases in invasive breast cancer. *Niger J Clin Pract* 2019, 22:63-68. doi:10.4103/njcp.njcp_198_18.
24. Park SI, Lee JH, Ham HJ, Jung YJ, Park MS, Lee J, Maeng LS, Chung YA, Jang KS: Evaluation of 2-[18F]-fluoro-2-deoxy-D-glucose positron emission tomography/computed tomography in rat models with hepatocellular carcinoma with liver cirrhosis. *Biomed Mater Eng* 2015, 26 Suppl 1:S1669-S1676. doi:10.3233/BME-151466.
25. Oya N, Nagata Y, Tamaki N, Takagi T, Murata R, Magata Y, Abe M, Konishi J: FDG-PET evaluation of therapeutic effects on VX2 liver tumor. *J Nucl Med* 1996, 37:296-302.
26. Kim JI, Lee HJ, Kim YJ, Kim KG, Lee KW, Lee JH, Lee HJ, Lee WW: Multiparametric monitoring of early response to antiangiogenic therapy: a sequential perfusion CT and PET/CT study in a rabbit VX2 tumor model. *ScientificWorldJournal* 2014, 2014:701954. doi:10.1155/2014/701954.

Figures

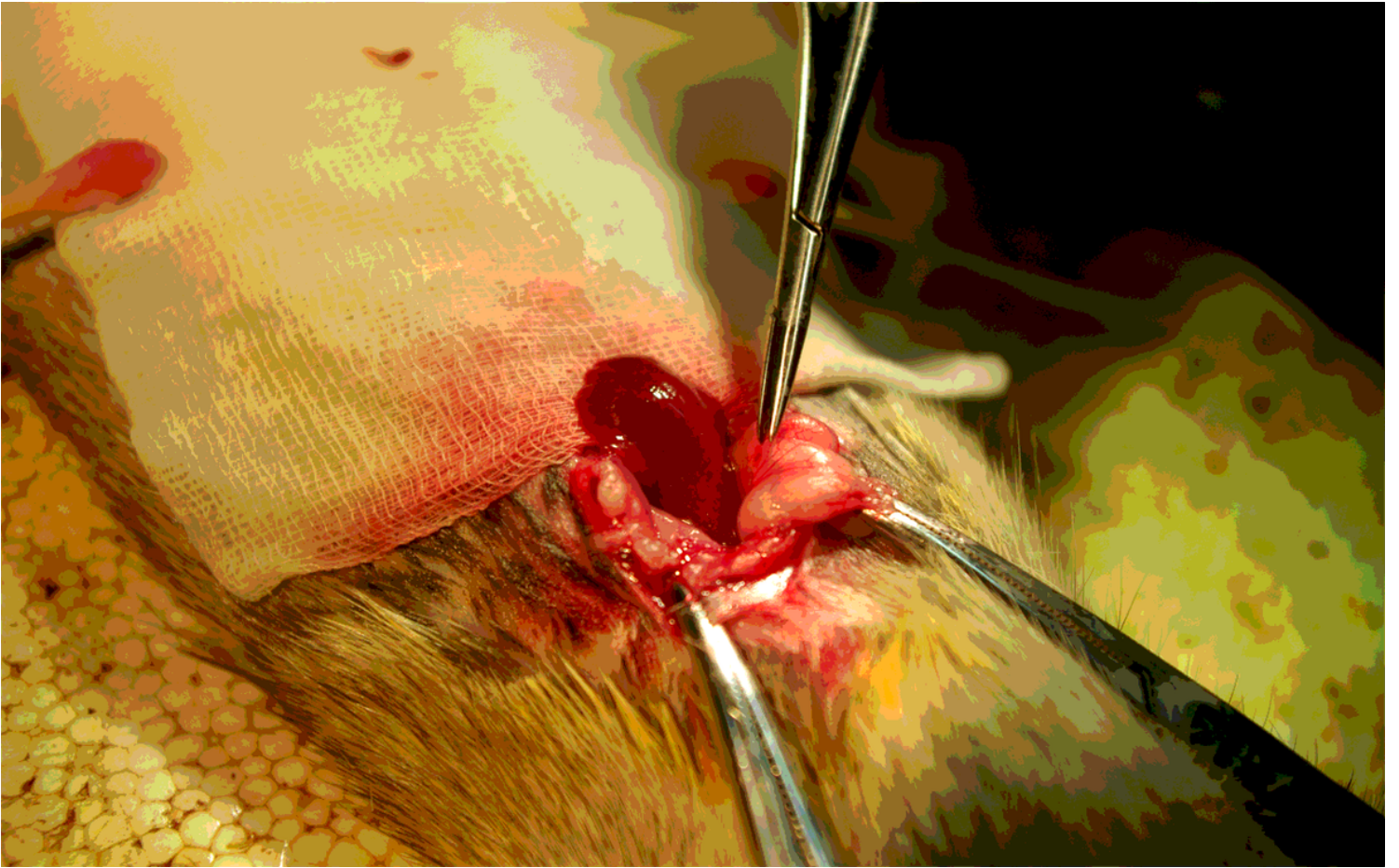


Figure 1

Plot illustrates the tumor implantation in the left lobe of rat liver

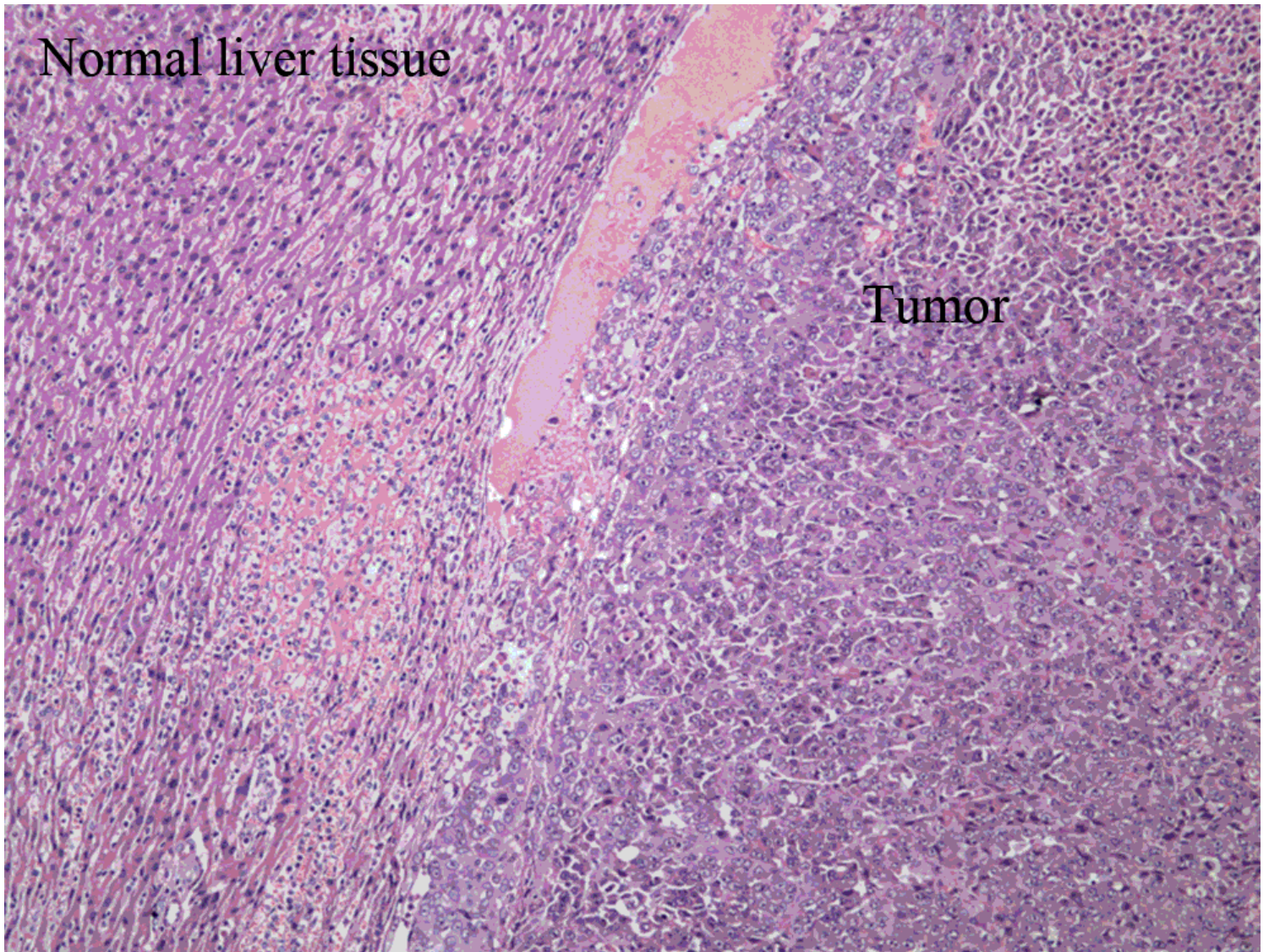


Figure 2

Plot illustrates the tumor and normal liver tissue. H&E X100

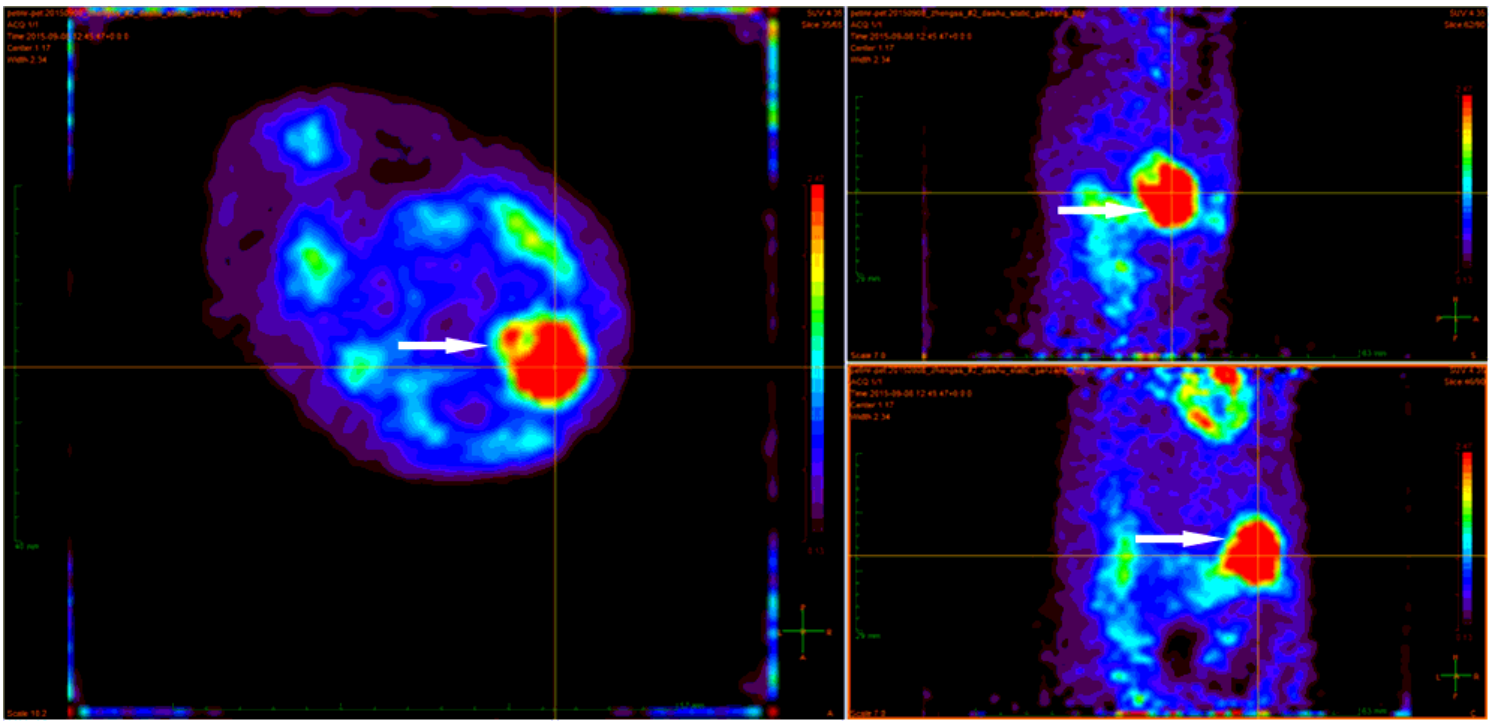


Figure 3

Plot illustrates a high uptake lesion by using the FDG-PET

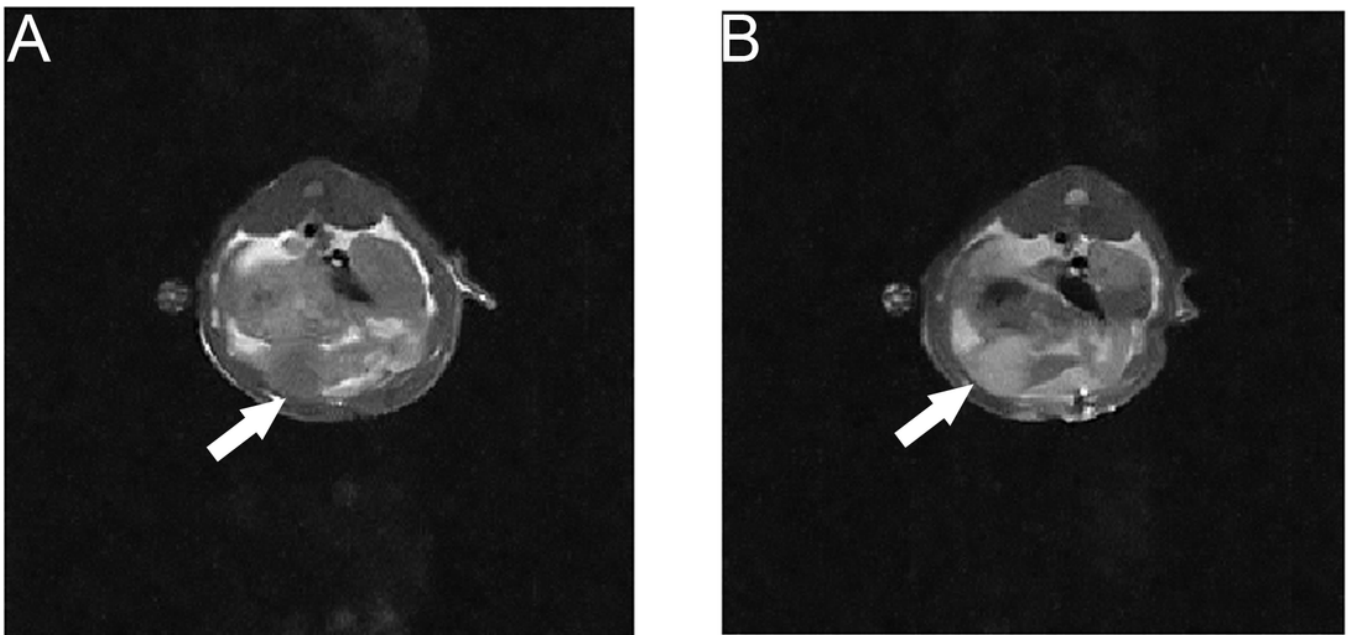


Figure 4

Plot illustrates MR imaging of the tumor. 14 days after the implantation, MR demonstrate a node with clear shape, hypointensity on T1-weighted (A) and hyperintensity on T2-weighted (B);